EFFECT OF TEMPERATURE ON ANTI-CORROSION PROPERTIES OF ALUMINUM ALLOY ANODIZED BY SULPHURIC ACID

Feyrouz NAFA,[a] Hakim BENSABRA,[b,*] Jean Paul CHOPART[c] and Mohamed Lyamine CHELAGMIA[d]

[a] Laboratory of Materials and Environment Interactions (LIME), University of Jijel, OuledAïssa, BP 98, Jijel 18000, Algeria
[b] Laboratory of Applied Energetics and Materials (LEAM), Université of Jijel, OuledAïssa, BP 98, Jijel 18000, Algeria
[c] MATIM Laboratory, UFR Sciences, University of Reims Champagne Ardenne, B.P. 1039 – 51687 REIMS (Cedex 2), France
[d] LAIGM Laboratoiry, 8 Mai 1945 University – Guelma, Algeria

Temperature is one of the most important parameters in anodizing treatments of aluminum alloys as it directly affects the quality of the anodic coatings. This research study has examined and investigated the effect of this important parameter on the anti-corrosion properties of the anodizing layers of aluminum alloy 5083. The morphology and crystalline structure of anodic oxide layers were characterized respectively by X-ray diffraction, scanning electron microscopy and EDX analysis. The corrosion behaviour of the alloy, before and after anodization at different temperatures, was analyzed in chlorinated medium using different electrochemical techniques, namely open circuit potential measurement, potentiodynamic polarization and electrochemical impedance spectroscopy. The results showed that temperature has a significant influence on the quality of the anodic oxide layers. Therefore, for a relatively low treatment temperature, the developed anodic films show high surface roughness values and contain fewer pores and defects compared to the films obtained at 20°C. Electrochemical analysis indicates that these films also show good corrosion resistance in the chloride environment. This is reflected by relatively low corrosion current density values as well as relatively high polarization resistance values.
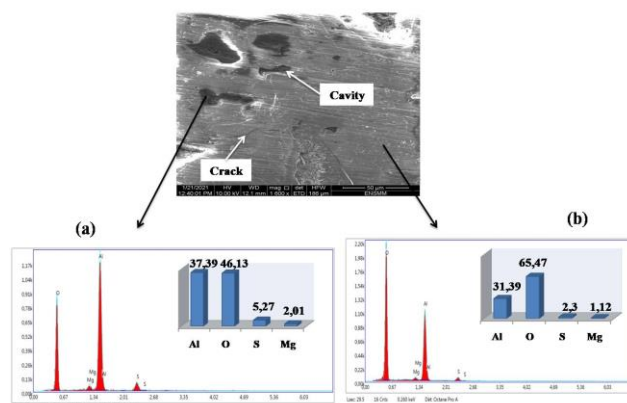
INTRODUCTION

Due to their low density and excellent mechanical properties, aluminium and its alloys remain the most widely used metallic materials in the industrial sector. They also find their application in several fields, namely mechanical engineering, aeronautics, architecture, automotive industry, maritime sector as a construction material, transportation, etc.[1] Compared with other metallic materials, especially cast iron and steel, aluminium alloys have good resistance to atmospheric corrosion, which is mainly caused by the formation of a stable and passive oxide layer that is tight and well adhered to the surface. However, in contact with aqueous media and especially in the presence of aggressive agents such as chlorides, this layer becomes thermodynamically unstable, and the metal loses its passivity which consequently undergoes localized corrosion attack. This form of corrosion usually results in the formation of more or less developed pits which significantly affects the serviceability properties of these alloys,

---

* Corresponding author: h.bensabra@univ-jijel.dz; tel.: +213792295013; fax: +21334501189

specifically the mechanical properties. To minimize the serious consequences of this mode of attack, the improvement of the corrosion resistance of this type of alloy has become more than necessary. Therefore, several prevention techniques have been implemented such as the use of corrosion inhibitors,[2-4] the application of organic and inorganic coatings,[5] and anodic oxidation, etc. Indeed, the anodizing treatment of aluminum and its alloys remains the most widespread protection technique because of its effectiveness and simplicity of application. It is an electrochemical surface treatment that allows the formation of anoxide layer (Al_2O_3)uniform, hard, protective and well adhered to the metal surface[6]. The properties of this oxide layer depend strongly on the experimental conditions of the anodizing treatment such as: the chemical composition of the electrolyte[7-9], current density[10], applied potential[11], processing time[12], and electrolyte temperature.

The temperature is a physical parameter of great importance in anodizing treatments; it mainly influences the metal dissolution rate, thickness and porosity of the formed film and consequently their different properties. This important factor has been the subject of several scientific research works which aim to study its effect on the different properties of anodized films. Dongchu *et al.* studied the influence of temperature (20-40°C) on the structure and growth mechanism of films prepared under the galvanostatic mode[13]. Similarly, F. Debuyck *et al.*[14], investigated the effect of temperature and the anodizing voltage on the porosity of the anodic oxide layer. This ensures that the temperature increase gives a higher porosity to the anodic film because of the temperature capacity, which expands the dissolution of the oxide in the acid electrolyte. In addition, S. Theohari et al. examined the effect of temperature on the anodizing treatment of Al-Mg alloy (5052) for porous film formation in comparison with pure aluminium[15]. The effect of different anodizing conditions (current density, electrolytic composition, and temperature) on the friction coefficient and Vickers hardness or microhardness of anodic oxide layers formed on two aluminium alloys was investigated[6].

Nevertheless, and despite the importance of this parameter and its direct influence on the quality of the anodic coatings, there are many limitations in the research studies of the effect of temperature on the anti-corrosion properties of these coatings. In this context, we have carried out this study with the main objective of defining the most adequate treatment temperature to obtain anodic coatings with high corrosion resistance. To do so, conventional anodizing treatments were applied to the 5083 aluminium alloy at different temperatures.

The obtained oxide layers were physicochemically characterized to evaluate the effect of temperature on their quality from a morphological point of view (presence and density of pores, thickness) followed by an electrochemical analysis using different electroanalytical techniques (measurement of the open circuit potential, potentiodynamic polarization and complex impedance spectroscopy) to evaluate the corrosion resistance in a chloride environment.

EXPERIMENTAL

1. Materials and sampling

The material used in this study is a 5083 aluminum alloy widely used in the chemical and marine industry[16]. The average chemical composition of this alloy is shown in Table 1.

2. Anodizing treatment

In this study, we have focused on a conventional anodization treatment which is the anodic oxidation in sulfuric acid. Before each treatment, the samples underwent a surface treatment including a mechanical polishing by series of silicon carbide emery papers of increasing grade (#320 to 1200°) and cleaning in acetone followed by a rinse with distilled water.

This mechanical stripping was followed by a chemical stripping according to the following consecutive steps:
– Degreasing in a mixture of 15/85(V/V) (volume ratio) concentrated nitric acid and phosphoric acid,
– Etching in 1M sodium hydroxide solution for 1 min at room temperature,
– Neutralizing in nitric acid (HNO_3) 30% (volume fraction) solution for 30 s,
– Rinsing with distilled water followed by air drying and stored in desiccators.

The anodization treatment of our alloy was carried out in a double-walled electrolysis cell connected to a thermostatic water bath allowing us to control the temperature of the treatment bath.

In this cell, the anode (Aluminium 5083) has an active surface of about 0.78 cm² and the cathode (aluminium alloy) has a larger surface, almost double, to increase the charge transfer surface. The two electrodes were immersed in the sulfuric acid solution (1M), separated by a distance of 1 cm.

The samples were anodized at a constant current density of 1.2 A/dm² in a sulphuric acid electrolyte (1M) for 60 min at different temperatures (5 and 20 °C).

3. Surface characterization

The thickness (e) and roughness (Ra) of the anodic oxide layers were measured using a CT 100 Non-contact profilometer (Cyber TECHNOLOGIE CT 100).The crystal structure of the anodized samples was analysed byX-ray diffraction (XRD) using a D8 Advance Brucker diffractometer (CuKα1, 2). Finally, the morphology and chemical composition of the oxide layers formed were examined using a scanning electron microscope coupled with an energy-dispersive X-ray analysis system (EDX) (FEI Quant).

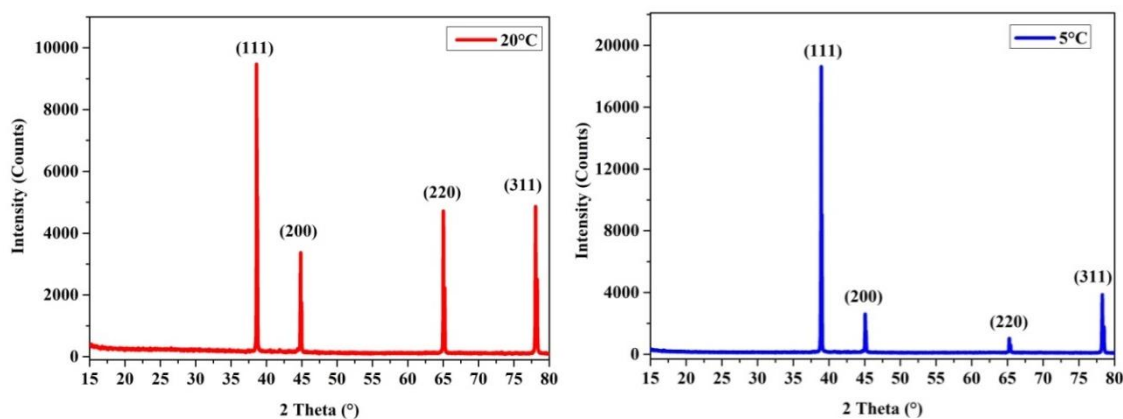| Element	Al	Mg	Mn	Cu	Fe	Cr	Zn	Ti	Si
Wt Pct	balance	4.93	0.33	0.15	0.10	0.10	0.05	0.04	0.02

Fig. 1 – Ray diffraction patterns on anodized samples at different temperatures.

4. Electrochemical analysis

The analysis of the electrochemical behaviour of the 5083 alloy, before and after anodization treatment at different temperatures, was carried out by means of different electrochemical analysis techniques, namely the measurement of the Open Circuit Potential (OCP), potentiodynamic polarization and impedance spectroscopy. The electrolytic medium used is a neutral chloride solution (3 wt% NaCl).

The tests of potentiodynamic polarization and electrochemical impedances were carried out using an assembly composed of a Potentiostat/Galvanostat of type Radio-Meter Analytical, model PGZ301, and a three-electrode cell system composed of saturated calomel electrode (SCE) as reference electrode, a platinum wire as counter electrode and the sample of anodized and not anodized aluminium alloy (5083) as the working electrode. The active surface was 0.78 cm^2.

The polarization curves were plotted in a potential range from -200 to +900 mV/ E_{corr} after one hour of immersion of the anodized and non-anodized samples in the chloride solution, the scan rate is 0.25 mV/s. The impedance spectra were plotted in the Nyquist plane for signal amplitude of 10 mV/E_{corr} and a frequency range of 100 kHz to 10 mHz. The experimental data obtained by plotting the EIS diagrams were fitted using ZsimpWin simulation software (version 3.30d).

RESULTS AND DISCUSSION

1. Morphological and structural analysis of anodized layers

The quality of the coatings obtained after anodic oxidation of aluminum alloys is intimately linked to the morphology and thickness of the oxide layer as well as the nature and proportion of chemical elements that compose it. In our work, the anodized samples were analyzed by X-ray diffraction and scanning electron microscope observations followed by an EDX analysis in order to highlight the effect of the anodization temperature on the properties of the anodized layers. Fig. 1 shows the XRD patterns of the oxide layers obtained by anodization at two different temperatures: 20 and 5°C.
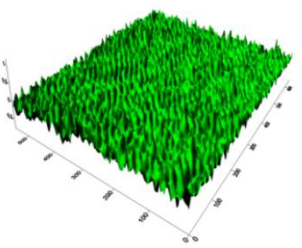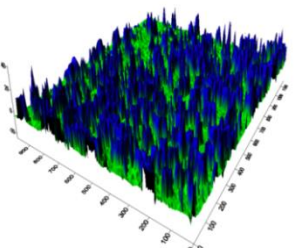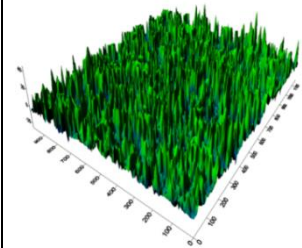
From the figure we can clearly see the existence of a clear difference between the intensities of the peaks of the obtained spectra. Thus, we note that the characteristic diffraction peaks at 38.55°, 44.82°, 65.25° and 78.43° are associated to the (111), (200), (220) and (311) planes of aluminum assigned to the cubic lattice structure. The absence of diffraction peaks attributed to the alumina phase (Al_2O_3) in the XRD spectra is due to the amorphous microstructure of the anodic films formed by conventional anodization[17].

We also note that the maximum intensity of the last three peaks decreases with the decrease of the electrolyte temperature; this means that, from a quantitative point of view, the amorphous coatings produced at 5°C are thicker compared to those formed at a temperature of 20°C. This was confirmed by profilometric measurements of the thickness of the layers, for example the thickness of the anodized layer at 5°C is 56.57 μm, whereas the layer obtained at 20°C is only 41.91 μm, Table 2.

From a morphological point of view, we have noticed that the layers anodized at 5°C are rougher than those obtained at a higher temperature. This is logical because the degree of roughness of the coatings increases with the increase of their thickness.

Table 2

The effect of anodizing temperature on the properties of the developed coatings

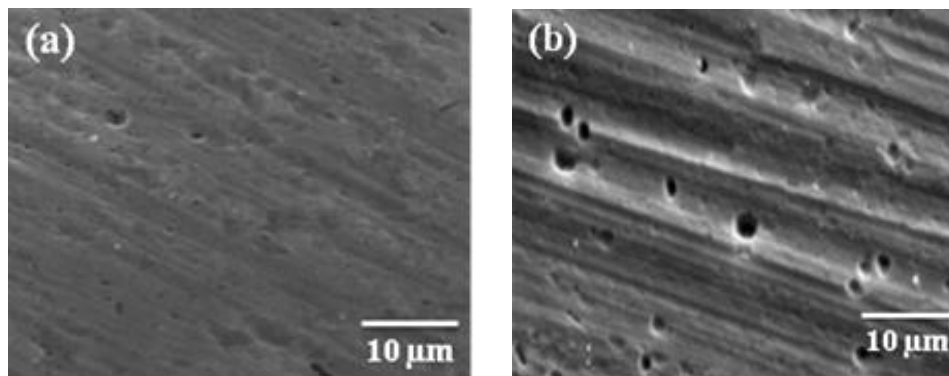|	Non-anodized	Anodized at 20 °C	Anodized at 5 °C
3D			
Ra (µm)	0.08	3.19	5.04
Coating Thickness (µm)	-	41.91	56.57

Fig. 2 – SEM images of anodic films obtained at different temperatures: (a) 5°C, (b) 20°C.

SEM observations have also confirmed the effect of the anodizing temperature on the quality of the layers from a morphological point of view. Thus, and according to Fig. 2b, the surface of the anodic film produced at 20°C presents numerous pores and cavities distributed in a random way, whereas the film produced at 5°C seems more homogeneous with a coarse structure presenting less pores and covering the whole metal surface. Thus, the change in passive film morphology resulting from the change in anodizing electrolyte temperature. AERTS *et al.*[18] consider that the increase in the temperature of the electrolyte causes an increase in the aggressiveness of the acid anodizing bath, which favors the chemical dissolution reaction of the forming anodic layer and leads to the formation of an anodic film with open pores.According to[19], the presence of these open pores is attributed to the evolution of oxygen during the formation of the oxide layer (Al_2O_3), to the cavities and cracks, Fig. 3, due to internal stresses as well as some local perturbations of the external region of the layer in formation.

The EDX spectra assigned to the anodized sample and the chemical composition estimated from these spectra are shown in Fig. 3. The analysis was carried out on two different points: the anodic oxide layer and the cavity level. Results obtained indicating the presence of the main chemical elements of the coatings: Al, O, Mg, and S. The presence of the first three species (Al, Mg, and O) can be attributed to the formation of Al_2O_3 and MgO oxides[20]. It has been shown that Mg^{2+} ions are added more rapidly to the oxide/electrolyte interface, allowing a uniform distribution through the oxide layer.

By comparing the estimated chemical composition from the two spectra obtained by the EDX analysis of the anodic oxide layer and at the cavity level it is shown that the latter contains a large quantity of sulfur to the anodic film, it goes from a value of 2.30 to a value of the order of 5.27 in % mass.

The presence of sulfur in the anodic film is explained by the migration of sulfate anions inward through the coating pores[21] during their growth. In addition,it is widely known that porous films formed

in sulfuric acid were contaminated by acid species (SO_4^{-2} ions)[22].The introduction of the SO_4^{2-} ion into the crystalline structure of the passive films leads to the formation of cracks in the passive aluminum films[23]. As a result, the quantity of oxygen in the cavities decreases, which leads to the appearance of any areas not covered by the Al_2O_3 film (discontinuity of the film), which alters the protective character of this film against wet corrosion, especially in the presence aggressive ions such as of chlorides.

2. Open circuit potential (OCP) measurements

The effect of the anodizing temperature on the evolution of OCP potential of the alloy in the chloride solution is expressed by the curves of Fig. 4.
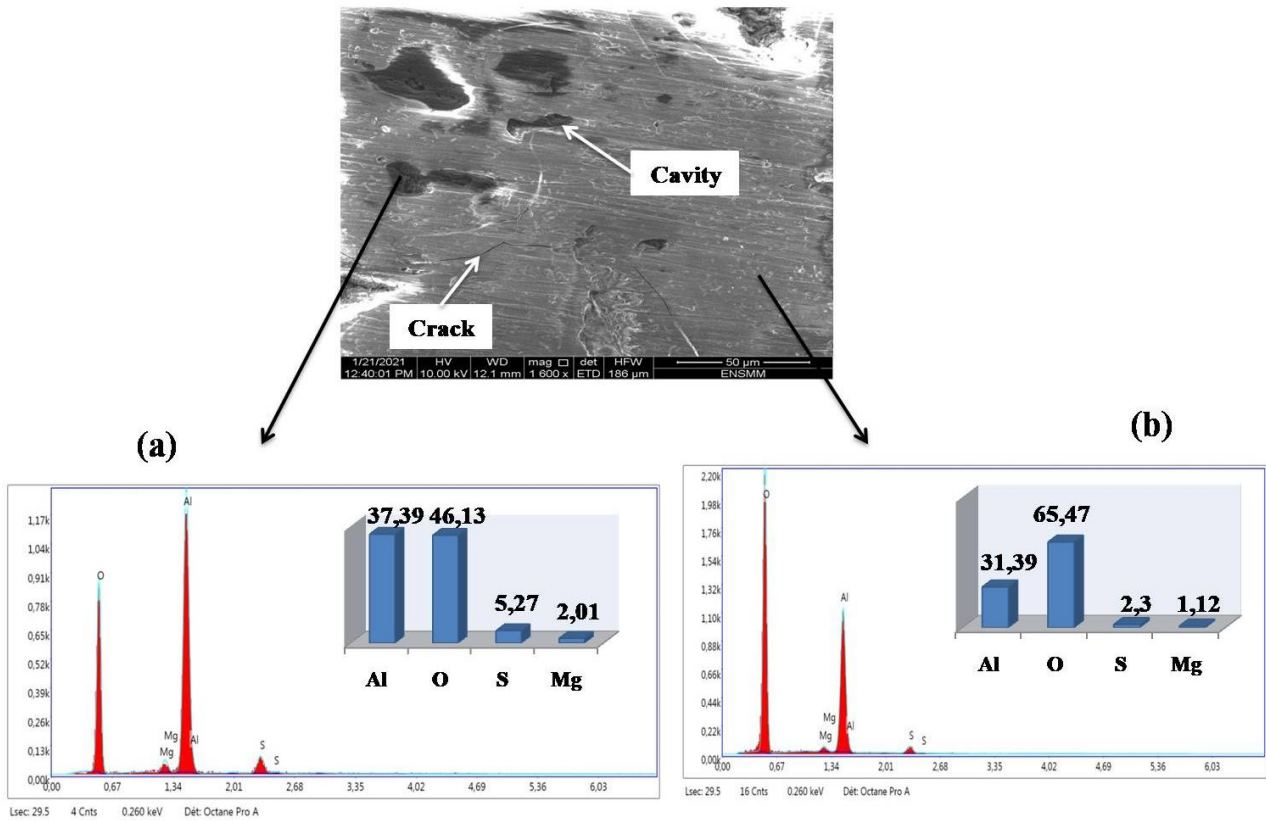

Fig. 3 – EDX analysis of the cavity level (a) and the anodic oxide layer (b) formed on Al 5083 in a sulfuric acid bath.
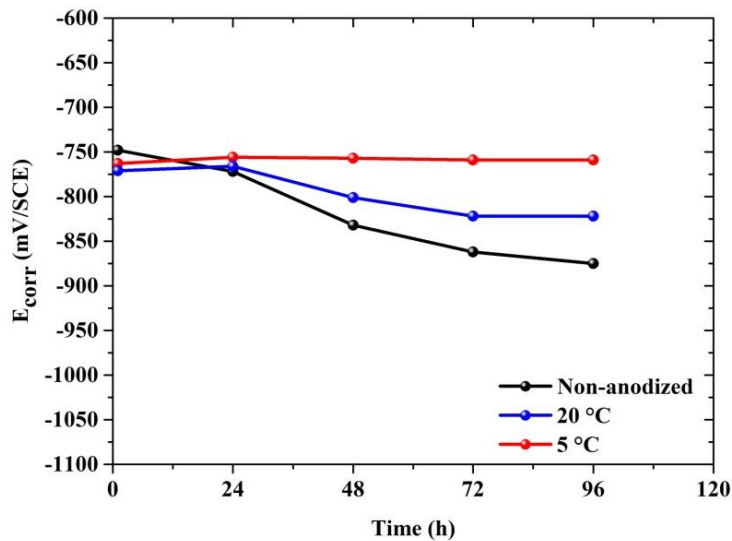

Fig. 4 – Effect of anodizing temperature on the OCP potential evolution.

The measurement of the OCP potential provides important preliminary informations on the electrochemical behavior of metals and alloys from a thermodynamic point of view in particular on the passivation mechanism: formation, stability and dissolution of passive films.

From the curves obtained, after a 96 h immersion in the chloride solution, we can easily see the significant effect of the anodizing temperature on the evolution of the free potential of 5083 aluminium alloy. Thus, we notice that for the non-anodized sample the corrosion potential follows a different evolution compared to the anodized samples especially in the first 24 hours of immersion: it becomes less and less noble with time and passes from a value of -748 mV/SCE at the beginning of the immersion to a value of -772 mV/SCE after an immersion time of 96 h. This evolution reflects, from a thermodynamic point of view, an electrochemical activity and a continuous dissolution of the alloy due to the chemical instability, under the action of chloride ions, of the passivation layer (Al_2O_3) naturally formed on the metal surface.

For the case of the samples anodized at 20 and 5°C we notice that for the first 24 hours of immersion the evolution of the free potential follows the same direction, the two samples present corrosion potentials which become more and more noble with time, this evolution reflects the electrochemical stability of the layer developed by anodic oxidation. However, after 24 hours of immersion in the solution, the potentials of the two samples evolve differently during the rest of the test period. Thus, the potential of the anodized sample at 20°C changes direction and becomes less and less noble with time, it passes from a value of -771 mV/SCE after 24 h of immersion to a value of about -766 mV/SCE after 96 h, while the potential of the anodized sample at 5°C still keeps its direction of evolution, it continues to take more and more cathodic values from the beginning of the immersion in a range going from -763 mV/SCE to -759 mV/SCE.

The difference in the evolution of the OCP potentials of the two samples reflects a different electrochemical behavior of the 5083 aluminium alloy, the anodization at a relatively high temperature (20°C) results in oxide layers less resistant to corrosion due to their chemical instability in the chloride medium. Anodizing at a low temperature (5°C) results in more stable oxide layers and more resistance to localized corrosion induced by Cl⁻ ions.

3. Potentiodynamic polarization

Potentiodynamic polarization, in spite of its destructive character, is a technique that provides important information about the electrochemical kinetics of corrosion reactions of metals and their alloys in different electrolytic media. The potentiodynamic polarization curves showing the corrosion behavior of the non-anodized and anodized alloy at different temperatures are presented in Fig. 5. The polarization curves were obtained in a 3% NaCl solution after an immersion time of 60 minutes.
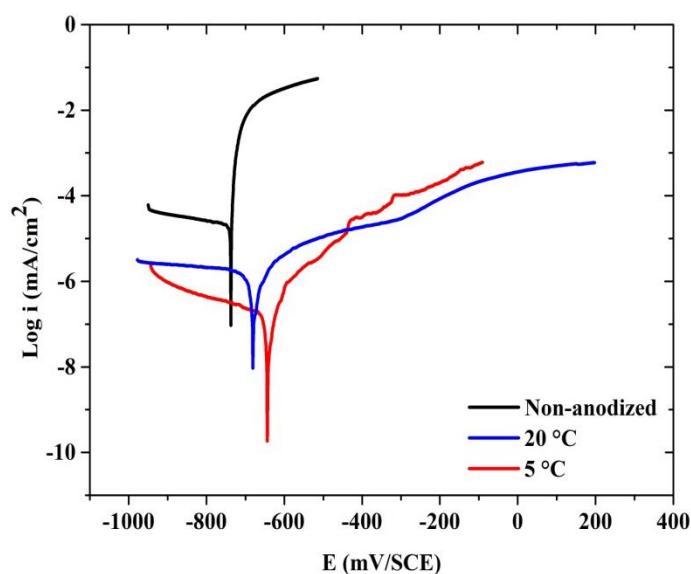

Fig. 5 – Polarization curves reflecting the anodizing temperature effect on the electrochemical behavior of 5083 aluminium alloy in chlorinated solution.

Evolution of electrochemical parameters with the anodizing temperature of 5083 aluminum alloy

	E_{corr} (mV/SCE)	i_{corr} (μA/cm^2)	V_{corr} (μm/y)	R_p (Kohm.cm^2)
Non-anodized	-739.2	21.1	229.84	0.33
20°C	-681.1	1.63	17.73	32.41
5°C	-643.4	0.29	3.16	202.89

From the obtained curves, we can see that the anodizing temperature has a significant influence on the electrochemical behavior of the anodized layers. Thus, we have to conclude the following: The non-anodized sample is, from an electrochemical point of view, much more active than the anodized ones at different temperatures, this activity is reflected by a less cathodic corrosion potential (E_{corr} = -739.2 mV/SCE) and a relatively high corrosion current density (i_{corr} = 21.1 μA.cm^{-2}); the current density begins to increase suddenly for a potential quite close to the corrosion potential (E_{corr}), this increase can be attributed to the formation and propagation of the pits[24] due to the chloride ions contained in the solution

The potentiodynamic polarization analysis revealed that the anodization treatment significantly improved the corrosion resistance of the alloy in the saline environment. The curves obtained indicate a remarkable decrease in the corrosion current density and a shift in the cathodic direction of the corrosion potential (E_{corr}). However, and according to the curves, we note a significant effect of the temperature on the corrosion resistance of the layers obtained by anodic oxidation. Thus, the sample anodized at low temperature (5°C) presents a better corrosion resistance reflected by a relatively low corrosion current density (i_{corr} = 0.29 μA.cm^{-2}) compared to the sample anodized at 20°C (i_{corr} =1.63 μA.cm^{-2}) and a more noble corrosion potential which is about -643.4 mV/ SCE,while that of the anodized sample at 20 °C is -681.1 mV/SCE. This difference in the behavior of the two samples can be attributed mainly to the morphological quality of the obtained oxide layers. The anodic oxidation at low temperature allows the formation of a thicker and more homogeneous oxide film with less defects (cavities and cracks), this film acts as a physical barrier between the aggressive solution and the metal substrate and thus prevents the diffusion of aggressive ions, primarily chloride ions.

The electrochemical parameters obtained from a Tafel plot by extrapolating the linear portion of the polarisation curvesare presented in Table 3.

4. Electrochemical impedance spectra

Electrochemical impedance spectroscopy has been recognized as one of the practical methods for determining characteristics and evaluating corrosion resistance of anodic oxide layers in aggressive environments[22, 25]. Figure 6 shows the Nyquist diagrams of the non-anodized and anodized samples at different temperatures after an immersion time of 24 hours in the chlorinated solution (3% NaCl).

From Fig. 6 we can see that all of the obtained spectra are formed by two semi-circular capacitive loops with two different time constants: a first loop at high frequencies (BHF) and a second at low frequencies (BBF). Due to the porous character of the anodization layers, the high frequency loop (BHF), which generally appears in the frequency range between 10^3 and 10^5 Hz, is often associated to the charge transfer phenomenon and the electrochemical double layer at the oxide/solution interface in the pores, while the BBF loop corresponds to the barrier layers. This model, adopted by various authors[26-28], seems quite representative for the phenomena occurring at this type of electrochemical interface (oxidized metallic surface/electrolytic solution).

The equivalent circuits proposed for the theoretical modeling of the obtained experimental results are shown in Fig. 7. This theoretical modeling allowed to simulate the electrochemical interface in both cases, non-anodized samples, Fig. 7a, and anodized samplesat two different temperatures (20 and 5°C), Fig. 7b, as well as to determine the values of the passive electrical elements for the characterization of the electrochemical behavior of the aluminium alloy.

As shown in Fig. 7a, the proposed circuit in the case of non-anodized aluminum is composed of a resistor R_e, which represents the resistance of the electrolyte in series with a first combination of two passive elements in parallel: a CPE_{dl} (Constant Phase Element) reflecting the capacitance of the double layer and a charge transfer resistor R_{ct} followed by a second combination formed by a CPE_f in parallel with a resistor R_f, attributed respectively to the capacitance and the resistance of the alumina film that is naturally formed on the metal surface.
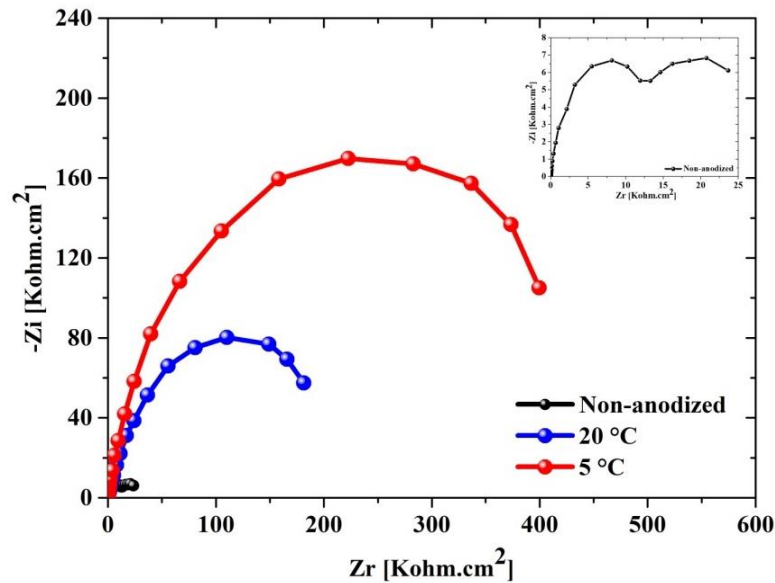
Fig. 6 – Impedance spectra reflecting the effect of the anodizing temperature on the behavior of 5083 aluminum alloy after 24 h of immersion in chlorinated solution.
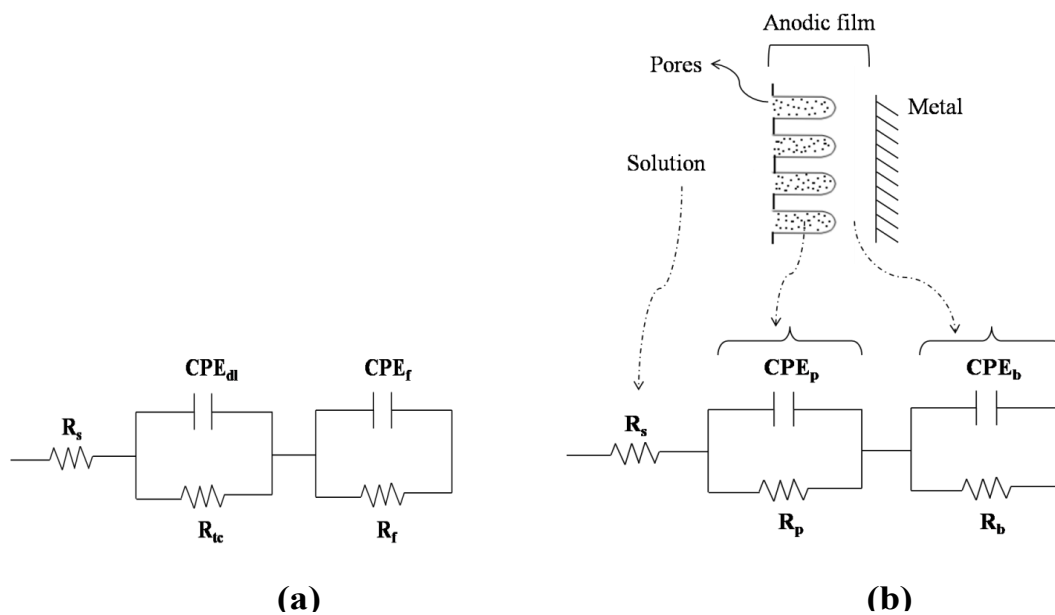

(a)   **(b)**

Fig. 7 – Corresponding equivalent circuits ofelectrochemical interface: (a) non-anodized alloy (b) anodized alloy.

Table 4

Calculated electrochemical parameters reflecting the chlorides effect on the electrochemical behaviour of non-anodized alloy

Time (h)	R_e (Kohm.cm^2)	CPE_{dc} (S.sα/cm^2)	n_1	R_{tc} (Kohm.cm^2)	CPE_f (S.sα/cm^2)	n_2	R_f (Kohm.cm^2)	Err (%)	χ^2
1	0.010	1.012 E-4	0.773	27.900	1.100 E-5	0.925	28.060	3.414	9.86 E-4
24	0.010	2.193 E-4	0.723	17.559	1.527 E-5	0.919	9.439	3.016	9.09 E-4

For the case of anodized aluminum the proposed equivalent circuit, Fig. 7b[29], consists of the same passive elements connected in the same way, however, in the first combination the CPE_p and the resistance R_p are attributed to the capacitance and the resistance of the porous layer, respectively, while in the second combination the phase constant element CPE_b and the resistance R_b characterize, respectively, the capacitance and resistance of the barrier layer.
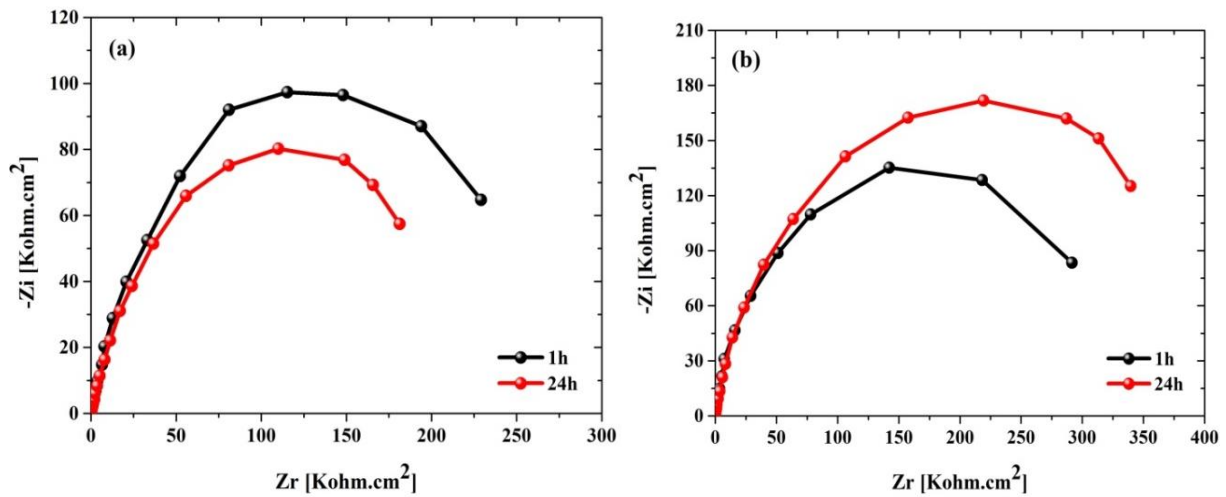
Fig. 8 – Impedance spectra of anodized aluminum at: (a) 20 °C, (b) 5 °C.

Table 5

Fitting result of EIS reflecting the effect of the anodizing temperature on the electrochemical behaviour of anodized alloy

	Temps (h)	R_e (Kohm.cm^2)	CPE_p (S.sα/cm^2)	n_1	R_p (Kohm.cm^2)	CPE_b (S.sα/cm^2)	n_2	R_b (Kohm.cm^2)	Err (%)	χ^2
20°C	01	0.012	4.466 E-5	0.711	0.670	5.876 E-6	0.826	203.30	3.496	1.22 E-3
	24	0.014	4.523 E-5	0.684	3.555	8.734 E-6	0.801	171.70	3.747	1.40 E-3
5 °C	01	0.011	2.647 E-6	0.887	155.40	1.026 E-5	0.889	172.30	8.325	6.93 E-3
	24	0.013	4.555 E-6	0.875	80.54	5.175 E-6	0.873	275.30	8.897	7.91 E-3

As for the two previous electrochemical analysis techniques (OCP measurements and potentiodynamic polarization), the electrochemical impedance spectroscopy allowed to highlight, on one hand, the beneficial effect of the anodization treatment on the corrosion behavior of aluminium alloy and the remarkable effect of the anodizing temperature on the quality of the anodic oxide layers on the other hand. Thus, and according to Fig. 6, we see that the Nyquist diagram obtained for non-anodized aluminum, after an immersion time of 24 hours in the saline solution, consists of two capacitive loops, BHF and BBF, of diameter smaller than that of the loops obtained for the anodized alloy (at 5 and 20°C). This reflects the electrochemical activity of aluminium alloy in the chloride medium, which is reflected in low values of the charge transfer resistance R_{tc} and the passive film resistance R_f and high values of the capacitance of two elements CPE_{dl} and CPE_f, Table 4. In fact, it is well known that in the case of the Nyquist plots, often used to evaluate electrochemical impedance data, the larger the

diameter of the semicircle loop, the better the corrosion resistance.[30]

For the anodized alloy, the EIS spectra indicate a significant improvement of the corrosion resistance in the chloride environment, which means that the anodic oxidation allowed obtaining passive oxide films, thicker, denser and therefore more electrochemically stable. Thus, and compared to the non-anodized alloy, the increase in the size of the capacitive loops, BHF and BBF, obtained in the case of the anodized alloy corresponds to a significant increase in the polarization resistance of the system joinyed to a decrease in the capacitance of the oxide films. As an indication, the film resistance increases from 9.439 in the case of the non-anodized alloy to 171.70 Kohm.cm^2 for the anodized alloy at 20°C, and in parallel to this increase the capacitance of the film passes from 1.527E-5 to 8.734E-6 S.sα/cm^2. As for the effect of the anodizing temperature, the impedance measurements confirm the notable effect of this important physical parameter on the corrosion resistance of the oxide layers obtained after treatment. From Fig. 6, we

see a clear difference between the diameters of the BHF and BBF capacitive loops obtained for the anodized alloy at two different temperatures. Thus, we note that the size of the loops obtained for the anodized alloy at 5°C is significantly higher than that of the loops obtained for the anodized alloy at 20°C. This difference in size, reflecting a greater corrosion resistance of the oxide layers developed at low temperature, is mainly attributed to the quality of these layers from a morphological point of view. These layers are thicker and have fewer pores, which makes them more impermeable and difficult to penetrate by aggressive agents, principally chloride ions.

Indeed, and as shown in Table 5, the improvement of the corrosion resistance of the anodic films obtained at 5°C is reflected by a marked increase of the values of R_p and R_b in parallel with a decrease of CPE_p and CPE_b. We observe that R_p goesfrom a value of 80.54 Kohm.cm² for the sample anodized at 5 °C to a value of 3.555 Kohm.cm² for the one anodized at 20 °C, as well as $R_b$which goes from 275.30 to 171.70 Kohm.cm^2 for the anodized films elaborated at 5 °C and 20 °C respectively. In conjunction with this increase we note a decrease in the values of CPE_p and CPE_b, Table 5 indicates that CPE_p increases from 4.555 E-6 S.sα/cm^2 for the sample anodized at 5 °C to 4.523 E-5 S.sα/cm^2 for the one anodized at 20 °C and CPE_b increases from a value in the range of 5.175 E-6 to 8.734E-6 S.sα/cm^2 for the samples anodized at 5 °C and 20 °C respectively. This improvement in corrosion resistance is also confirmed by the decrease in n values, it goes from 0.875 in the case of anodization at 5 °C to a value of 0.684 in the case of the film formed at 20 °C, this decrease indicates that the film/electrolyte interface is becoming more heterogeneous, moreover indicates the formation of new corrosion products.

One of the most important characteristics of the passive films is the stability with time, so to verify the reliability of the developed coatings we have compared the Nyquist spectra obtained for two different immersion times in the saline solution: 1 and 24 hours. The results obtained are shown in Figs. 8a (20 °C) and 8b (5 °C).

From the spectra presented on the figures we observe a clear difference in the corrosion behaviour over time of the two samples. Thus, the Nyquist diagrams of Fig. 8a, corresponding to the anodic film developed at 5°C, show that the latter becomes more and more stable with time, this stability is expressed by the increase of the diameters of the capacitive loops with time which corresponds to a clear improvement of the corrosion resistance of the alloy reflected by an increase in the values of R_p and R_b joint to a decrease in the values of the capacity of the two phase constant elements CPE_p and CPE_b, Table 5. On the other hand, the Nyquist diagrams obtained for the anodized alloy at 20°C, Fig. 8a, indicate an evolution of the corrosion resistance completely opposite to that of the anodized alloy at 5°C, *i.e.*, the anodic film obtained at 20°C is less stable, it becomes more and more active with time, this electrochemical activity is revealed by a significant decrease of the diameters of the capacitive loops over the time. This difference in stability with time or reliability of the layers is mainly due to the quality of the two anodized layers: the increase in the corrosion resistance of the barrier layer of the film produced at 5°C with time reveals that this layer has not been attacked by chloride ions because of its high compactness. This is in agreement with the results of V. Moutarlier *et al.* who claim that the less porous surface improves the corrosion resistance by restricting the penetration of chlorides in the passive film[22]. As for the layer elaborated at high temperature, its low chemical stability in time is principally attributed to the presence of a large number of pores and their size, this is due to the fact that the high temperature makes the anodizing electrolyte more aggressive which favors the dissolution of the oxidizing film which prevents the obtaining of a thick and more compact film. Indeed, the presence of pores not only facilitates the penetration and diffusion of chloride ions towards the surface, which leads to a localized breakage of the passive layer, but also can play the role of oxygen reservoirs, which accelerates the oxidation mechanism of the aluminum exposed at these points.

CONCLUSION

Through this research we have tested the influence of temperature on the morphology and structure of the oxide layers obtained by anodization of the alloy Al 5083 and consequently on its corrosion behavior in saline environments. At the end of our work, we have to conclude the following:

Physicochemical surface analysis has shown that the oxide layers obtained after anodizing at low temperature (5°C) are thicker and denser (contain fewer pores and microcracks) compared to the layers obtained at relatively high temperature (20°C). This is due to the fact that the exaggerated temperature activates the dissolution of the oxide film formed during the anodization process, which prevents it from growing properly.

The electrochemical characterization showed that the corrosion behavior of the alloy in a chloride environment was significantly affected by the quality of the developed anodic layers. Thus, the anodic films elaborated at low temperature show a much better corrosion resistance than those obtained at high temperature. This improvement in resistance was reflected in a significant decrease in corrosion current density and an anoblissement of free potential over time, as well as an increase in the polarisation resistance of the oxide film in conjunction with a decrease in capacitance according to the impedance spectra.

The improved corrosion resistance of low temperature anodized films is attributed to the quality of these films from a structural and morphological point of view as well as from a chemical stability point of view. Their good sealing and thickness make them sufficiently insulating physical barriers between the metal surface and the aggressive solution, which significantly impedes the diffusional mechanism of the aggressive agents.

REFERENCES

1. J. Wang, S. Huang, H. Huang, M. He, P. Wangyang and L. Gu, *J. Alloys. Compd.*, **2019**, *777*, 94.
2. H. Cen, X. Zhang, L. Zhao, Z. Chen and X. Guo, *Corros. Sci.*, **2019**, *161*, 108197.
3. W. Liu, A. Singh, Y. Lin, E. E. Ebenso, L. Zhou and B. Huang, *Int. J. Electrochem. Sci.*, **2014**, *9*, 5574.
4. M. Acila, H. Bensabra and M. Santamaria, *Metall. Res. Technol.*, **2021**, *118*, 203.
5. R. E. Klumpp, U. Donatus, R. M. P. da Silva, R. A. Antunes, C. D. S. C. Machado, M. X. Milagre, J. V. de Sousa Araujo, B. V. G. de Viveiros and I. Costa, *Surf. Interface. Anal.*, **2021**, *53*, 314.
6. M. Guezmil, W. Bensalah, A. Khalladi, K. Elleuch, M. Depetris-Wery and H. Ayedi, *Trans. Nonferrous. Met. Soc. China.*, **2015**, *25*, 1950.
7. K. Morshed-Behbahani, P. Najafisayar, R. Hessam and N. Zakerin, *Metall. Mater. Trans A.*, **2020**, *51*, 5475.
8. R. Elaish, M. Curioni, K. Gowers, A. Kasuga, H. Habazaki, T. Hashimoto and P. Skeldon, *Surf. Coat. Technol.*, **2018**, *342*, 233.
9. M. L. Mopon, J. S. Garcia, D. M. Manguerra and C. J. C. Narisma, *Coatings.*, **2021**, *11*, 405.
10. S.-J. Lee and S.-J. Kim, *Appl. Surf. Sci.*, **2019**, *481*, 637.
11. W. J. Stępniowski, M. Norek, M. Michalska-Domańska, A. Bombalska, A. Nowak-Stępniowska, M. Kwaśny and Z. Bojar, *Appl. Surf. Sci.*, **2012**, *259*, 324.
12. B. D. Mert, B. Yazici, T. Tüken, G. Kardaş and M. Erbil, *Prot. Met. Phys. Chem.*, **2011**, *47*, 102.
13. J. Li, H. Wei, K. Zhao, M. Wang, D. Chen and M. Chen, *Thin Solid Films*, **2020**, *713*, 138359
14. F. Debuyck, M. Moors and A. Van Peteghem, *Mater. Chem. Phys.*, **1993**, *36*, 146.
15. S. Theohari and C. Kontogeorgou, *Appl. Surf. Sci.*, **2013**, *284*, 611.
16. A. V. Jebaraj, K. Aditya, T. S. Kumar, L. Ajaykumar and C. Deepak, *Mater. Today: Proc.*, **2020**, *22*, 1470.
17. M. M. Ali and S. Sathiya, *Curr. Sci.*, **2020**, *234*, 118.
18. T. Aerts, T. Dimogerontakis, I. De Graeve, J. Fransaer and H. Terryn, *Surf. Coat. Technol.*, **2007**, *201*, 7310.
19. S. Ono, H. Ichinose and N. Masuko, *J. Electrochem. Soc.*, **1991**, *138*, 3705.
20. X. Zhou, G. Thompson, P. Skeldon, G. Wood, K. Shimizu and H. Habazaki, *Corros. Sci.*, **1999**, *41*, 1599.
21. K. Shimizu, H. Habazaki, P. Skeldon, G. Thompson and G. Wood, *Electrochim. Acta*, **2000**, *45*, 1805.
22. V. Moutarlier, M. Gigandet, L. Ricq and J. Pagetti, *Appl. Surf. Sci.*, **2001**, *183*, 1.
23. M. Michalska-Domańska, M. Norek, W.J. Stępniowski and B. Budner, *Electrochim. Acta*, **2013**, *105*, 424.
24. E. MaCafferty, *Corros. Sci.*, **2003**, *45*, 1421.
25. R. G. Kelly, J. R. Scully, D. W. Shoesmith and R. G. Buchheit, "Techniques in Corrosion Science and Engineering", New York: Marcel Dekker, Inc, 2003.
26. V. Moutarlier, M. Gigandet, J. Pagetti and L. Ricq, *Surf. Coat. Technol.*, **2003**, *173*, 87.
27. V. Moutarlier, M. Gigandet, B. Normand and J. Pagetti, *Corros. Sci.*, **2005**, *47*, 937.
28. B. Usman, F. Scenini and M. Curioni, *J. Electrochem. Soc.*, **2020**, *167*, 041505.
29. F. Mansfeld, *Electrochim. Acta*, **1993**, *38*, 1891.
30. S. Joshi, W. G. Fahrenholtz and M. J. O'Keefe, *Surf. Coat. Technol.*, **2011**, *205*, 4312.